Electronic Supplementary Material (ESI) for RSC Advances.

Supplementary information

The Synthesis of a ^{99m}Tc-Labeled Tetravalent Targeting Probe upon Isonitrile Coordination to $^{99m}Tc^{I}$ for Enhanced Target Uptake in Saturable Systems

Yuki Mizuno[†, ‡], Tomoya Uehara[†], Chun-wei Jen[†], Hiromichi Akizawa[‡*], and Yasushi Arano[†]

[†] Laboratory of Molecular Imaging and Radiotherapy, Graduate School of Pharmaceutical Sciences, Chiba University, 1-8-1 Inohana, Chuo-ku, Chiba 260-8675, Japan

[‡] Laboratory of Physical Chemistry, Showa Pharmaceutical University, 3-3165 Higashi-Tamagawagakuen, Machida, Tokyo 194-8543, Japan

HPLC methods. A L-7100 (Hitachi Ltd, Tokyo, Japan) equipped with a L-7405 UV detector (monitoring at 254 nm or 220 nm) and a NaI(TI) radio-detector (Gabi star, Raytest Strubenhardt, Germany) were used for high performance liquid chromatography (HPLC).

Preparative RP-HPLC was performed with a Cadenza 5CD-C18 (20 × 150 mm, Imtakt Co., Kyoto, Japan) connected to a Cadenza 5CD-C18 guard cartridge (10 × 8 mm, Imtakt Co.) at a flow rate of 5 mL/min with a mobile phase starting from 45% solvent A (0.1% TFA/water) and 55% solvent B (0.1% TFA/MeOH) to 40% solvent A and 60% solvent B at 45 min (system 1) or starting from 50% solvent A (0.1%TFA/water) and 50% solvent B (0.1%TFA/MeOH) to 40% solvent A and 60% solvent B at 45 min (system 2) or starting from 50% solvent A (0.1%TFA/water) and 50% solvent B (0.1%TFA/MeOH) to 25% solvent A and 75% solvent B at 40 min (system 3) or starting form 90% solvent A (Water) and 10% solvent B (MeCN) to 82.5% solvent A and 17.5% solvent B at 30 min to 100% solvent B at 35 min (system 4) or with a Cadenza CW-C18 (10 × 150 mm, Imtakt Co.) at a flow rate of 3 mL/min with an isocratic mobile phase of 56.5% solvent A (0.1% TFA/water) and 43.5% solvent B (0.1% TFA/MeOH) (0-30 min), followed by linear gradient over 5 min to 100% solvent B (system 5).

Analytical RP-HPLC was performed with a Cadenza 5CD-C18 (4.6 × 150 mm, Imtakt Co.) at a flow rate of 1 mL/min with a mobile phase starting from 50% solvent A (0.1% TFA/water) and 50% solvent B (0.1% TFA/MeOH) to 40% solvent A and 60% solvent B at 25 min to 100% solvent B at 27 min (system 6) or starting from 50% solvent A (0.1% TFA/water) and 50% solvent B (0.1%

TFA/MeOH) to 25% solvent A and 75% solvent B at 25 min to 100% solvent B at 27 min (system 7) or with an isocratic mobile phase of 70% solvent A (0.1% TFA/water) and 30% solvent B (0.1% TFA/MeOH) (0-5 min), followed by linear gradient over 10 min to 100% solvent B (system 8) or with a Cadenza CW-C18 (4.6 × 150 mm, Imtakt Co.) at a flow rate of 0.7 mL/min with a mobile phase starting from 57% solvent A (0.1% TFA/water) and 43% solvent B (0.1% TFA/MeOH) to 52% solvent A and 48% solvent B at 20 min to 100% solvent B at 25 min, followed by an isocratic mobile phase of 100% solvent B for 2 min (system 9) or starting from 90% solvent A (Water) and 10% solvent B (MeCN) to 75% solvent A and 25% solvent B at 20 min (system 10) or starting from 59% solvent A (0.1%TFA/water) and 41% solvent B (0.1% TFA/MeOH) to 54% solvent A and 46% solvent B at 20 min to 100% solvent B at 25 min, followed by an isocratic mobile phase of 100% solvent B for 2 min (system 11).

Scheme S1. Synthesis of L_β' (8a), L_G' (8b), and L_G (16)[a]

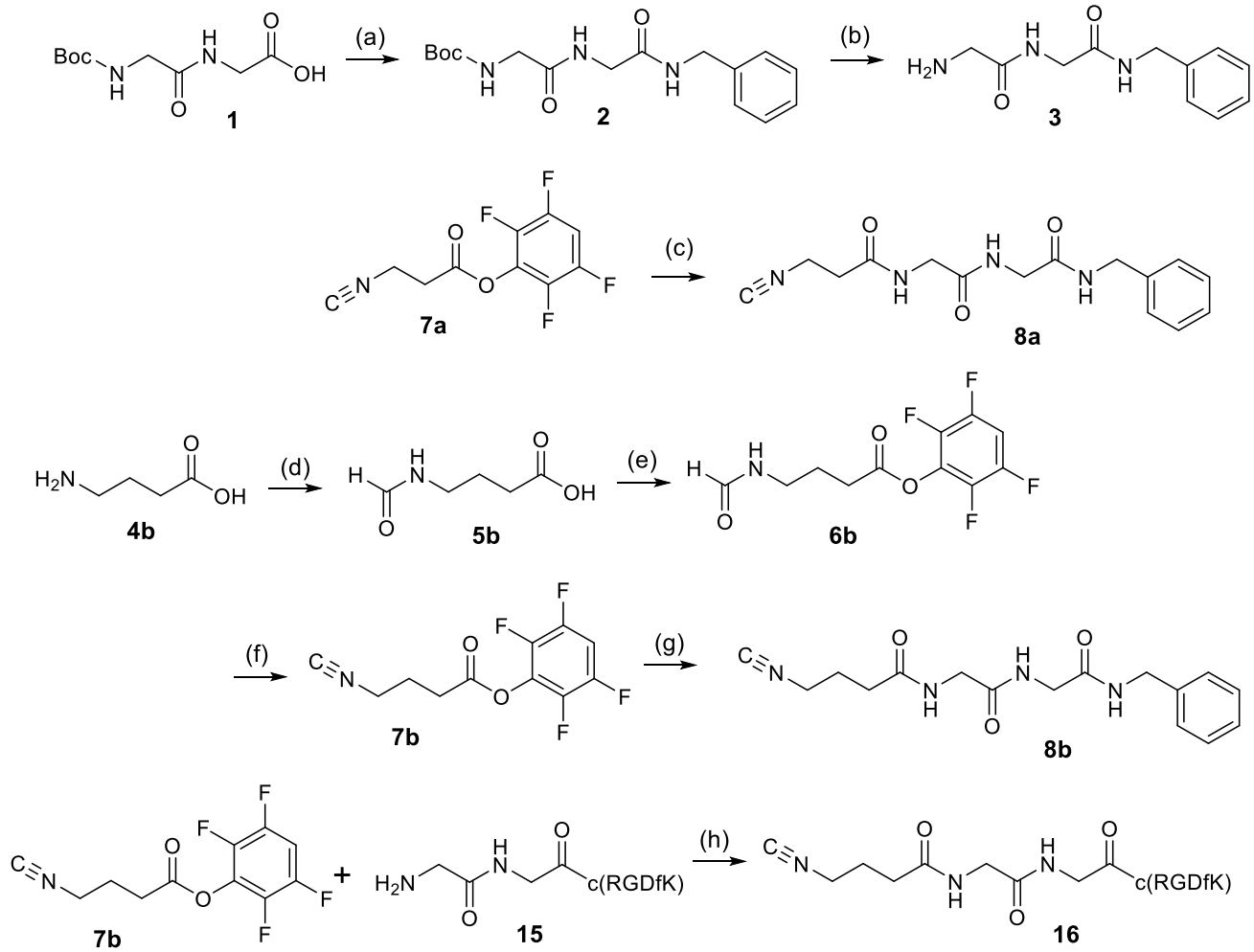

[a]Reagents and conditions: (a) benzyl amine, EDC·HCl, $CHCl_3$, 76%; (b) TFA; (c) compound **3**, $NaHCO_3$, DMF, 72%; (d) formic acid, acetic anhydride, 39%; (e) 2,3,5,6-tetrafluorophenol, EDC·HCl, $CHCl_3$, 83%; (f) Burgess reagent, CH_2Cl_2, 60%; (g) compound **3**, $NaHCO_3$, DMF, 63%; (h) $NaHCO_3$, DMF, 52%.

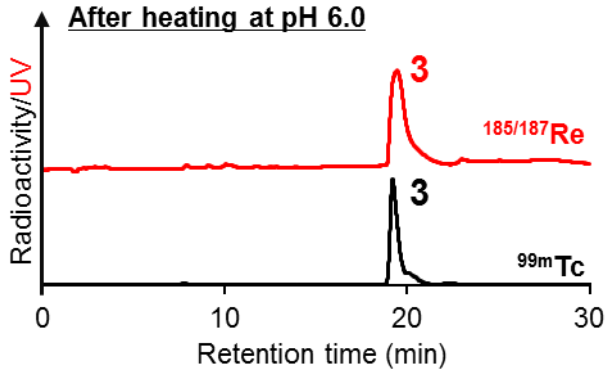

Figure S1. HPLC analyses (system 6) of M-[L_{β}']$_3$ (M = $^{185/187}$Re and ^{99m}Tc) after heating at 100°C for 30 min at pH 6.0. M-[L_{β}']$_3$ remained intact after the heating.

Table S1. In vitro stability of ^{99m}Tc-[L_G]$_4$ in 10 mM histidine solution and murine plasma[a]

time (h)	percent of intact	
	10 mM Histidine	Murine Plasma
1	98.5 ± 0.2	99.1 ± 0.1
6	98.1 ± 0.2	98.7 ± 0.4

[a]Results are expressed as mean ± SD of three experiments. Percent of intact was determined by TLC analysis.

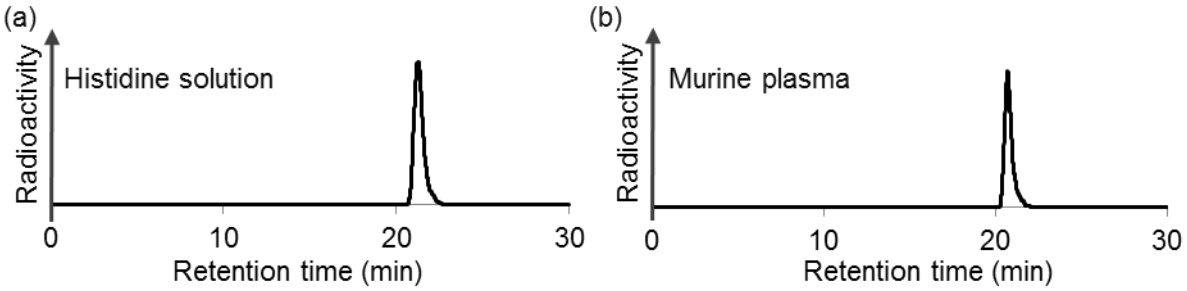

Figure S2. In vitro stability of ^{99m}Tc-[L_G]$_4$ in histidine solution and murine plasma. HPLC analysis after 6 h incubation (a) in 10 mM histidine solution and (b) in murine plasma. Plasma proteins were precipitated with EtOH prior to HPLC analysis.

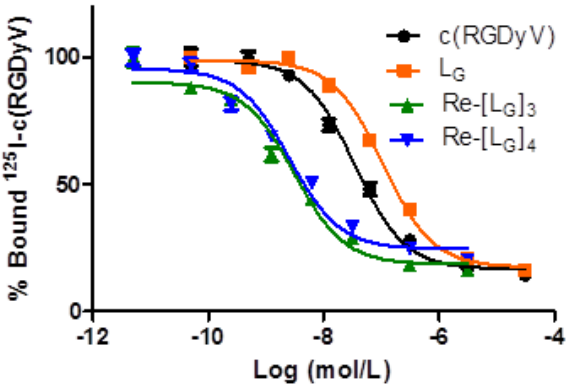

Figure S3. In vitro inhibition curves of ^{125}I-c(RGDyV) bound to U87MG glioma cells by L_G, Re-[L_G]$_3$, Re-[L_G]$_4$, and c(RGDyV) at 37 °C.

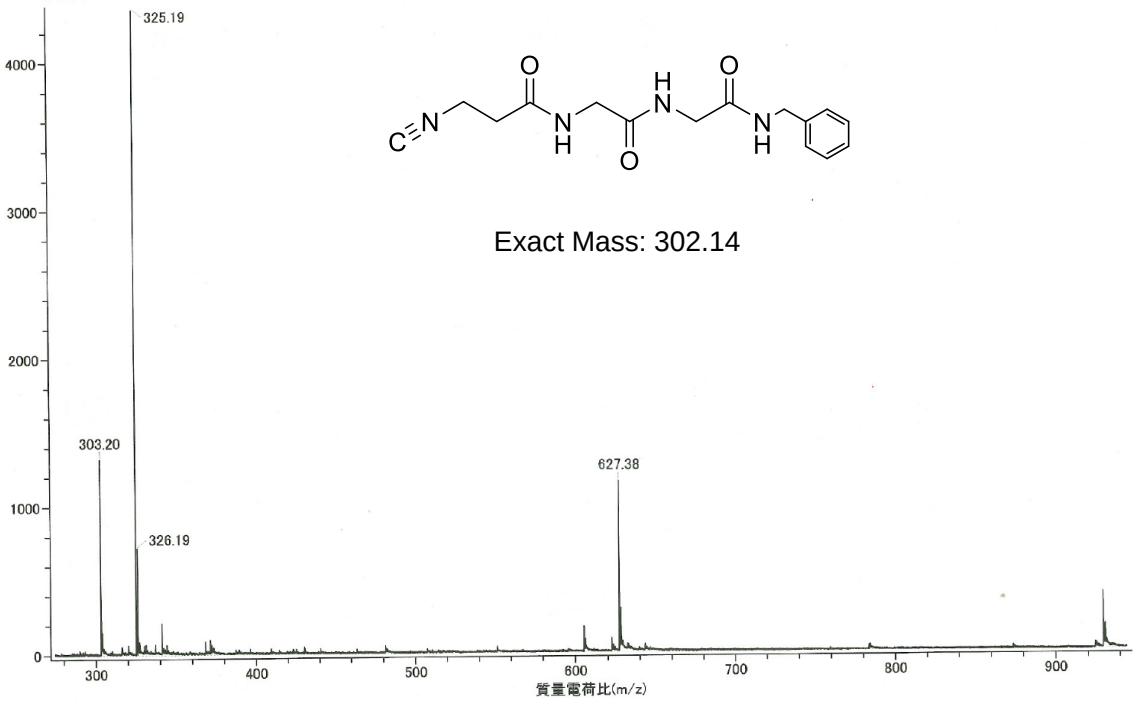

Figure S4a. ESI-MS spectrum of Lβ' (**8a**).

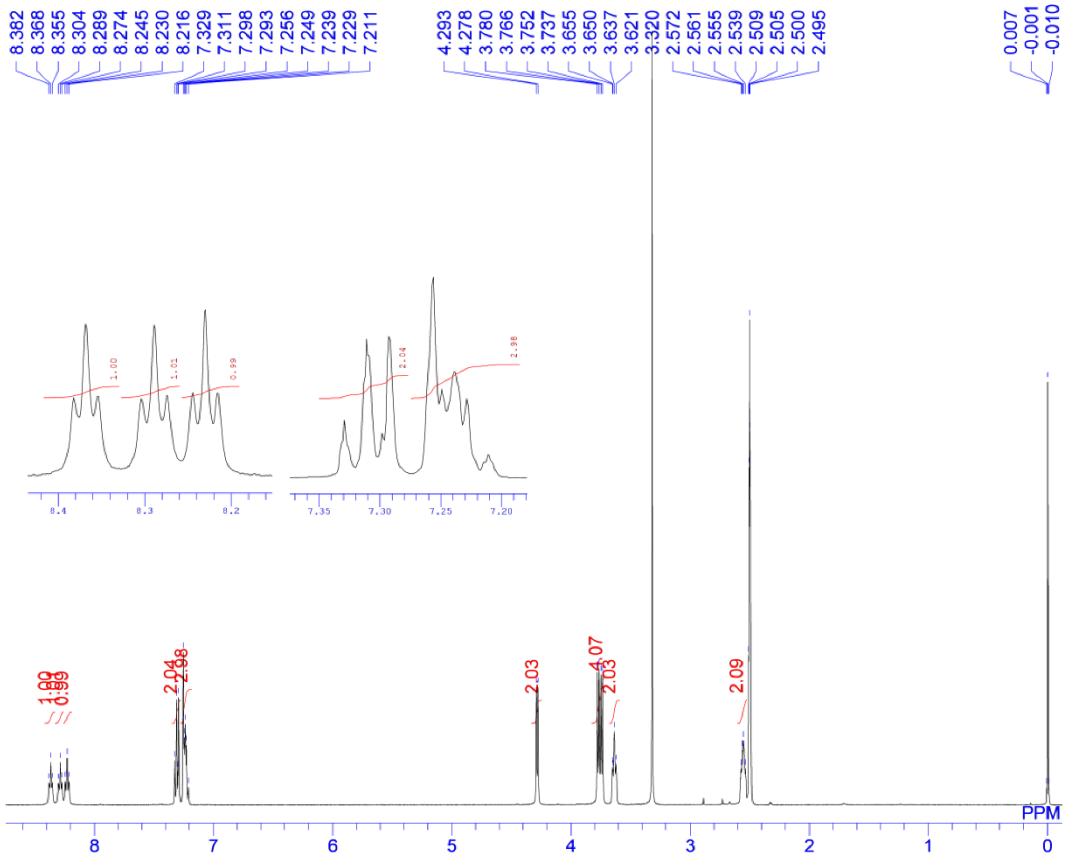

Figure S4b. ^{1}H NMR spectrum of Lβ' (**8a**) in DMSO-d_6.

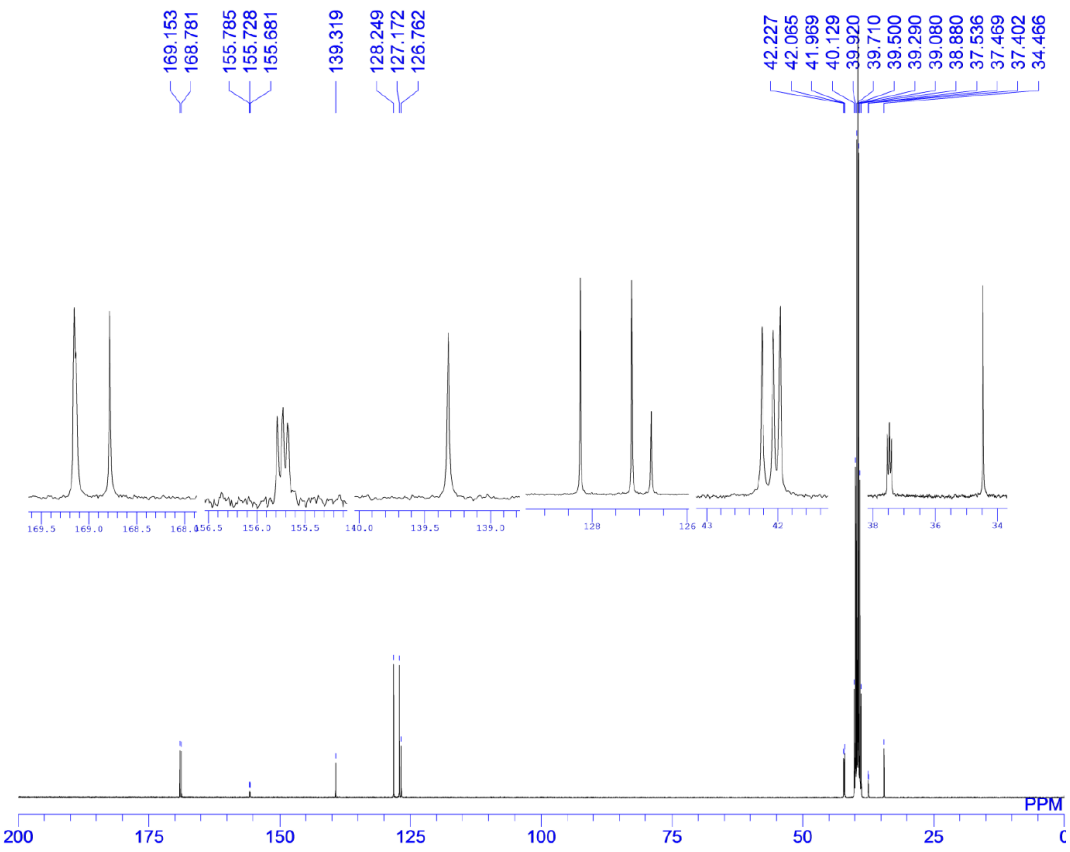

Figure S4c. ^{13}C NMR spectrum of L_{β}' (**8a**) in DMSO-d_6.

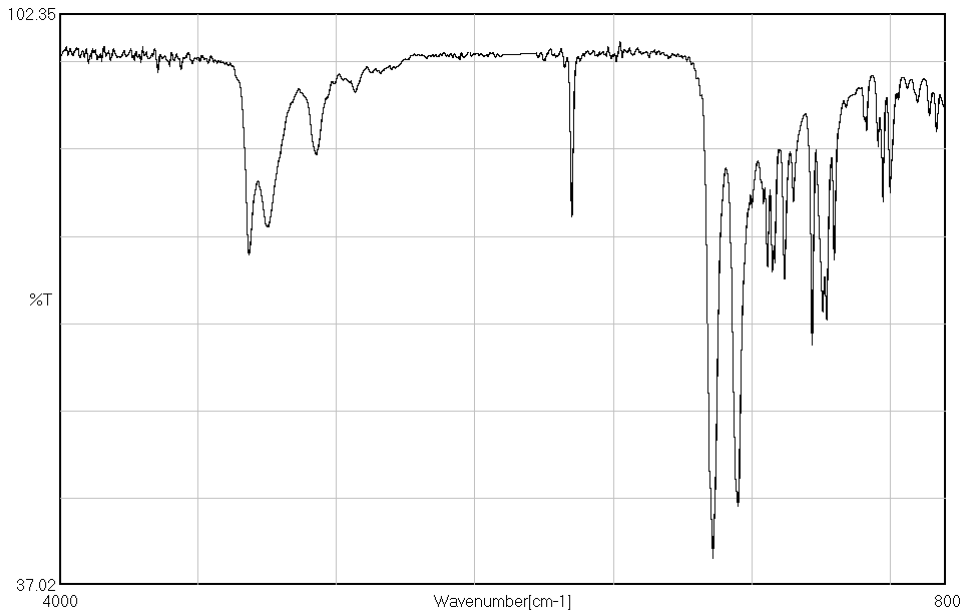

Figure S4d. IR spectrum (ATR) of L_{β}' (**8a**).

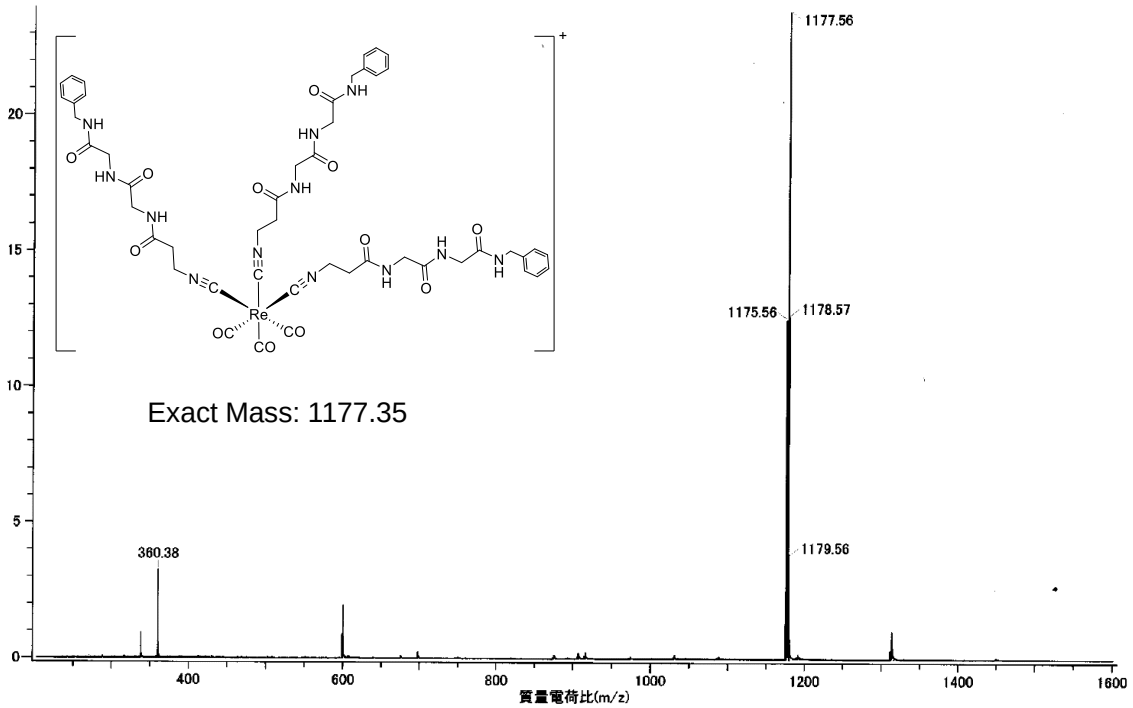

Figure S5a. ESI-MS spectrum of $[^{185/187}Re(CO)_3(L_\beta')_3]^+$ (**9**).

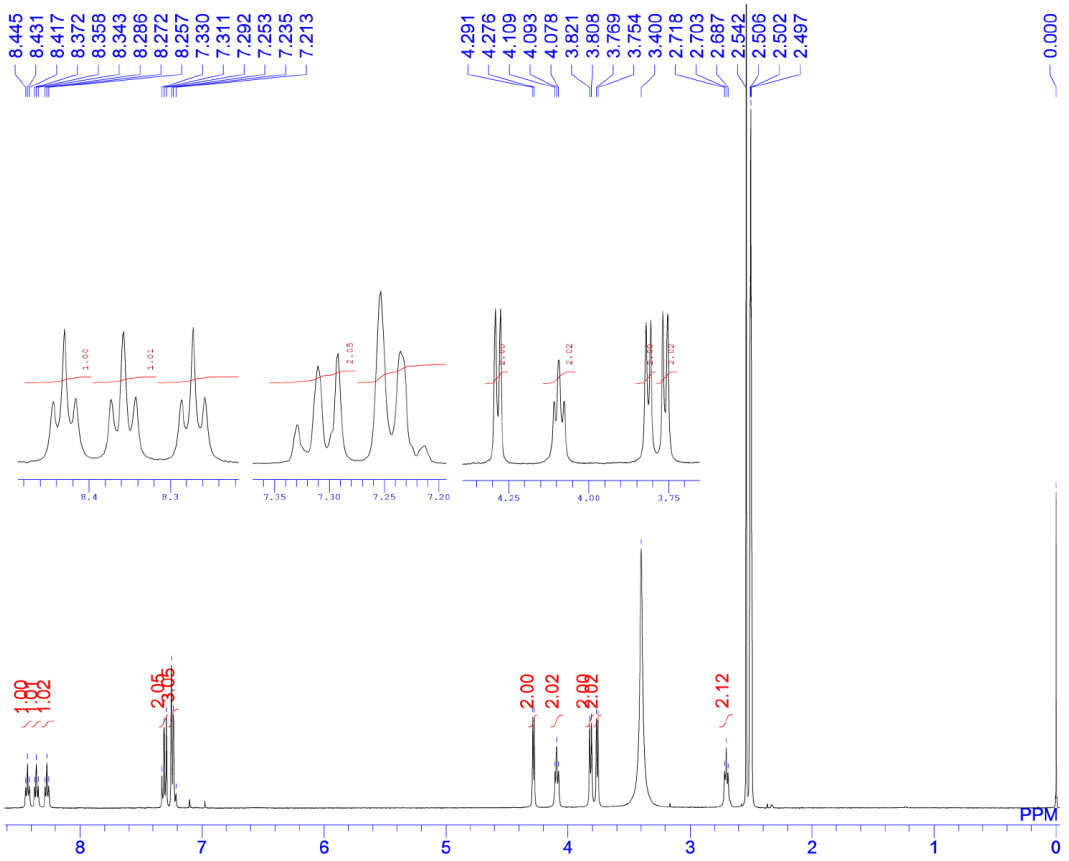

Figure S5b. ^{1}H NMR spectrum of $[^{185/187}Re(CO)_3(L_\beta')_3]^+$ (**9**) in DMSO-d_6.

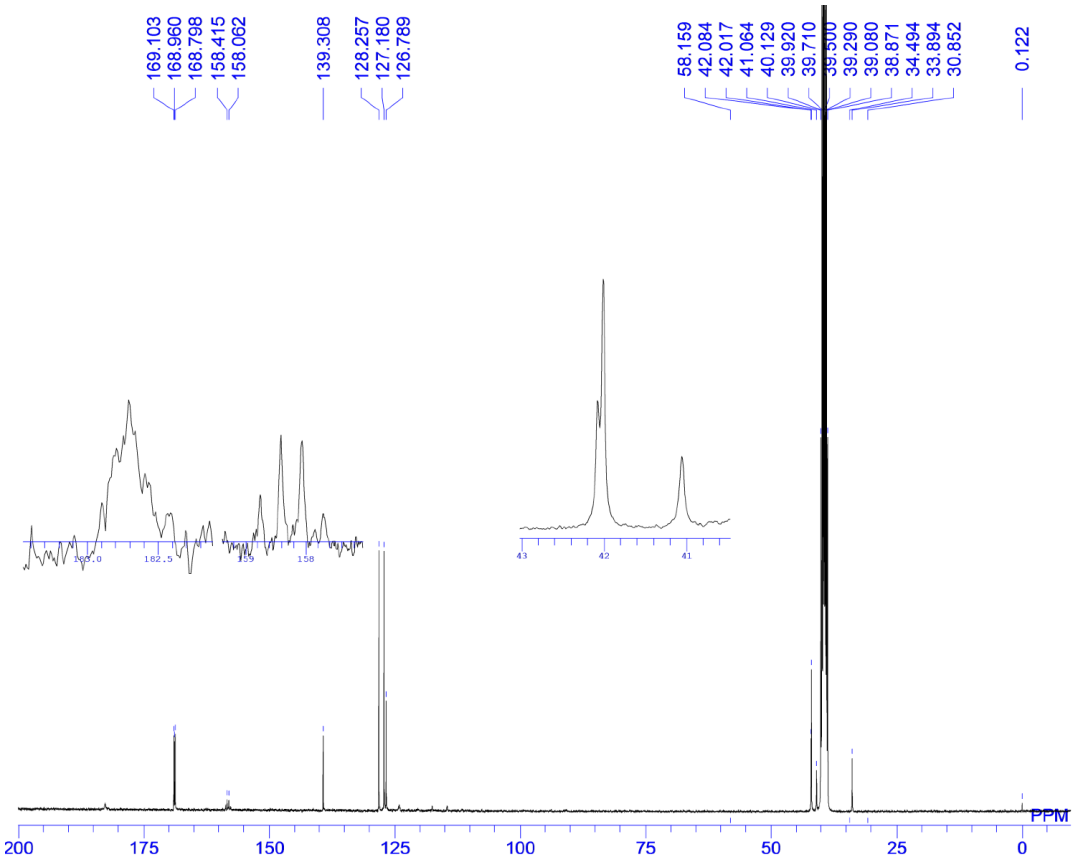

Figure S5c. ^{13}C NMR of $[^{185/187}Re(CO)_3(L_{\beta}')_3]^+$ (**9**) in DMSO-d_6.

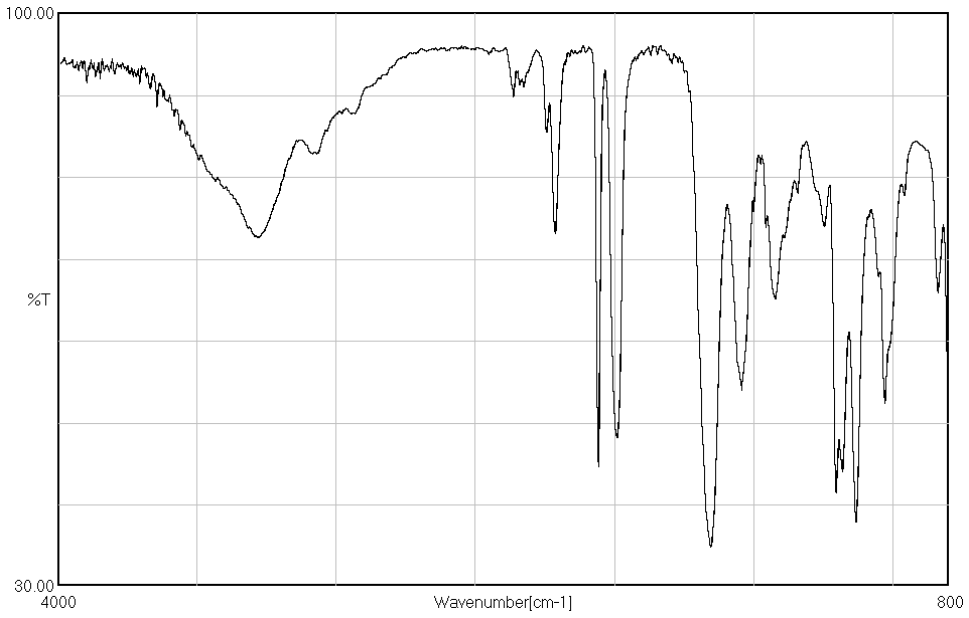

Figure S5d. IR spectrum (ATR) of $[^{185/187}Re(CO)_3(L_{\beta}')_3]^+$ (**9**).

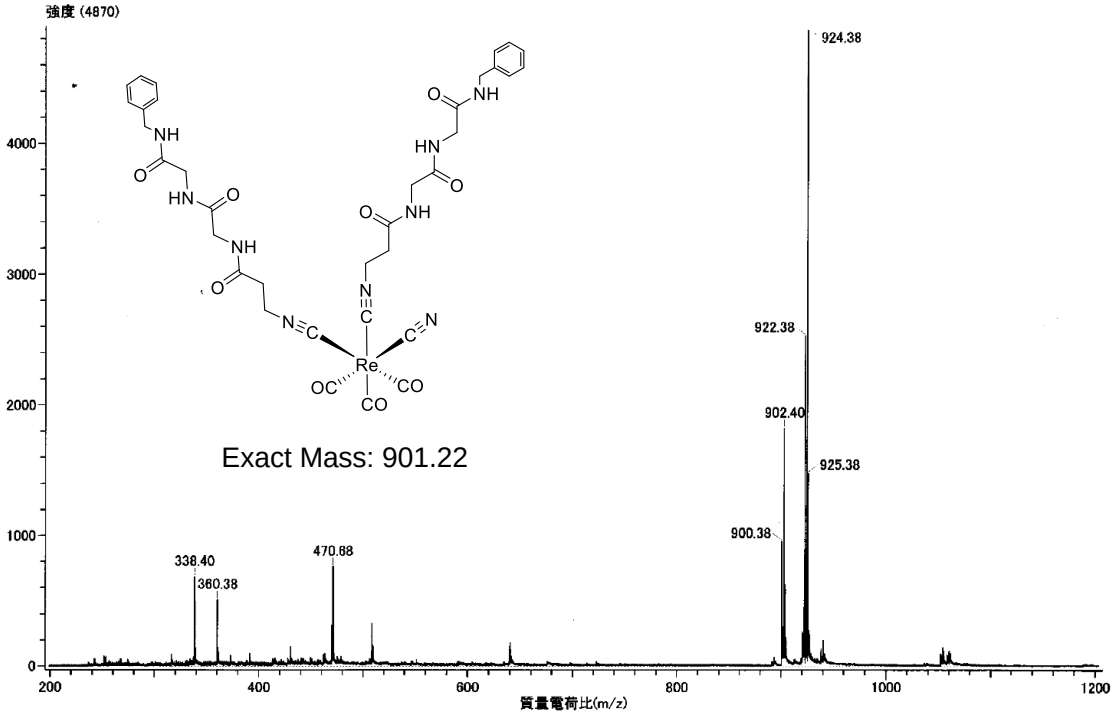

Figure S6a. ESI-MS spectrum of [$^{185/187}$Re(CO)$_3$(CN)(L$_\beta$')$_2$] (**13**).

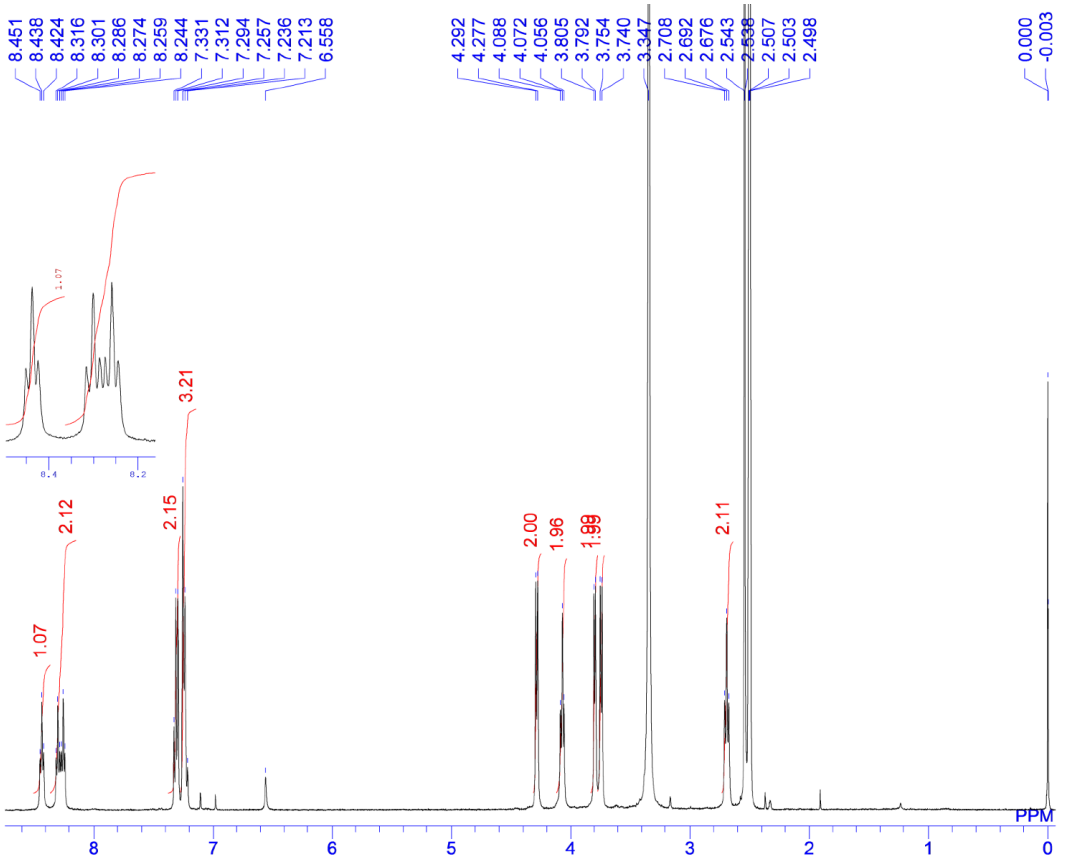

Figure S6b. ^{1}H NMR spectrum of [$^{185/187}$Re(CO)$_3$(CN)(L$_\beta$')$_2$] (**13**) in DMSO-d_6.

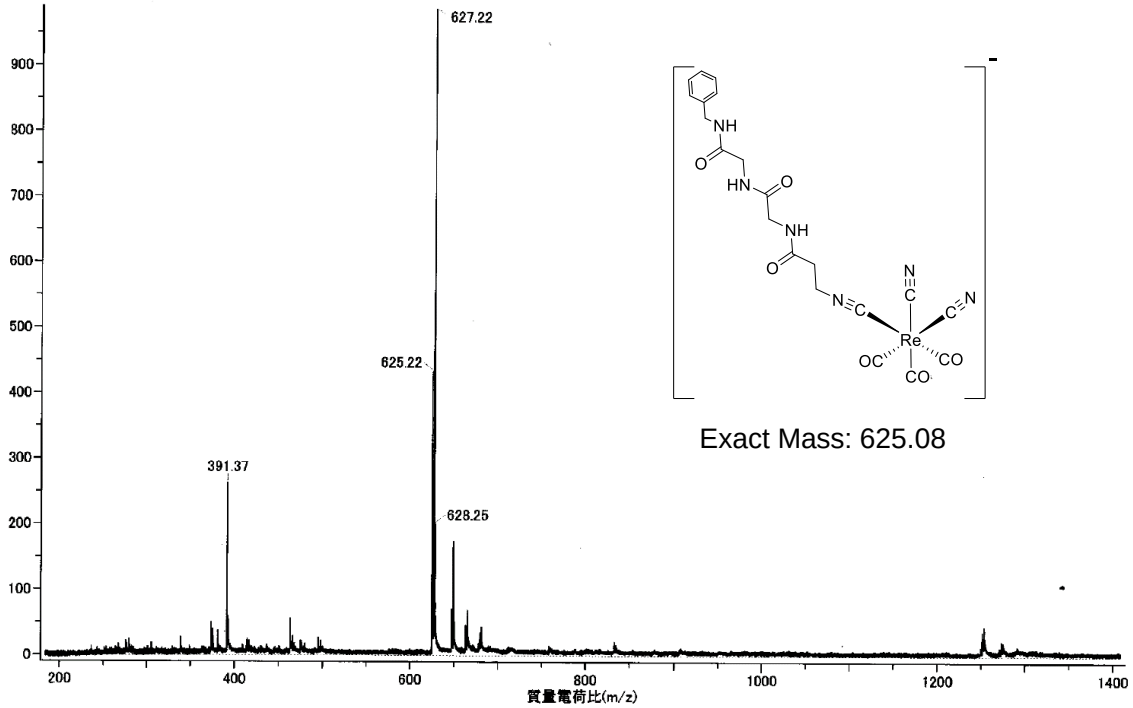

Figure S7a. ESI-MS spectrum of $[^{185/187}Re(CO)_3(CN)_2(L_{\beta}')]^-$ (**14**).

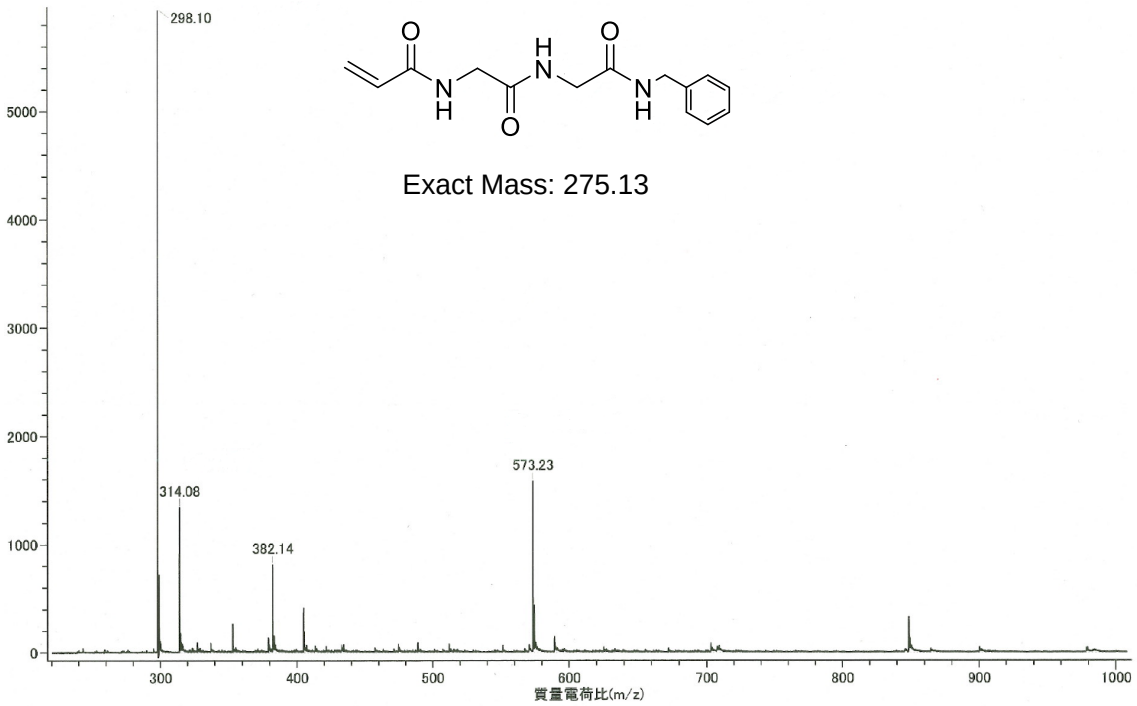

Figure S8a. ESI-MS spectrum of the eliminated ligand (**12**).

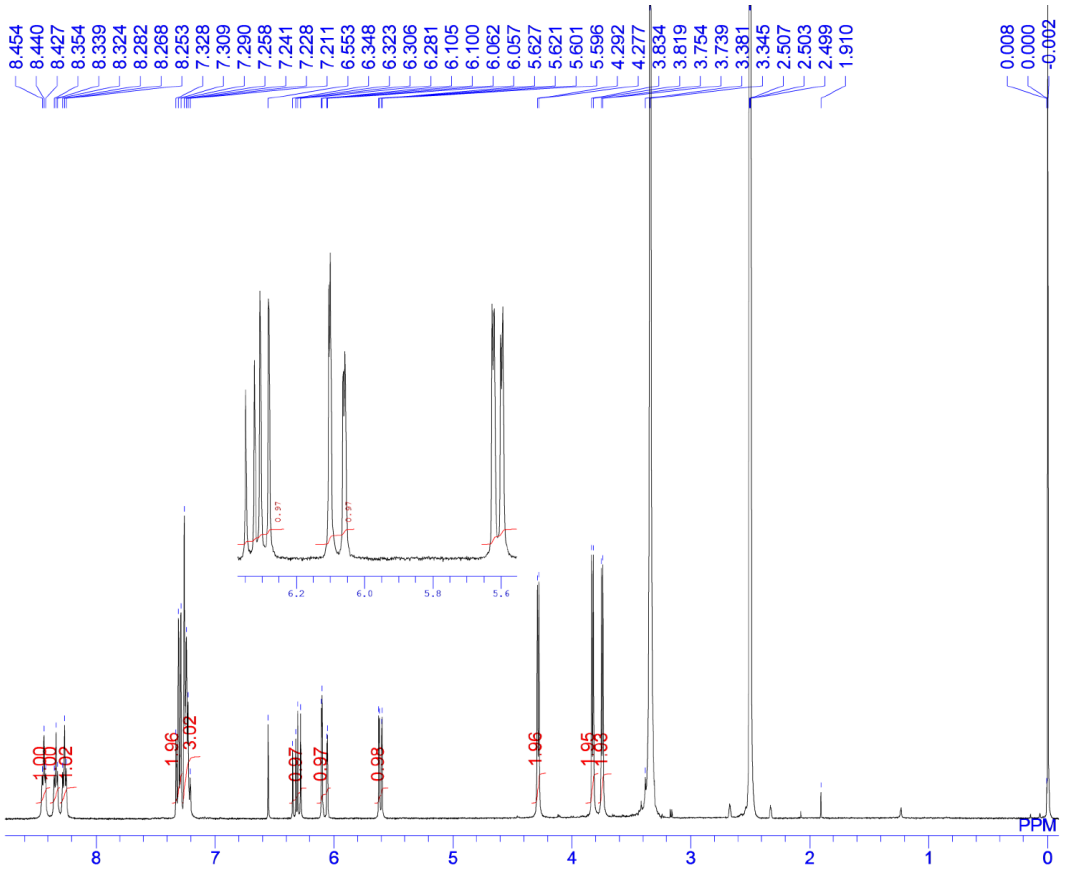

Figure S8b. ^{1}H NMR spectrum of the eliminated ligand (**12**) in DMSO-d_6.

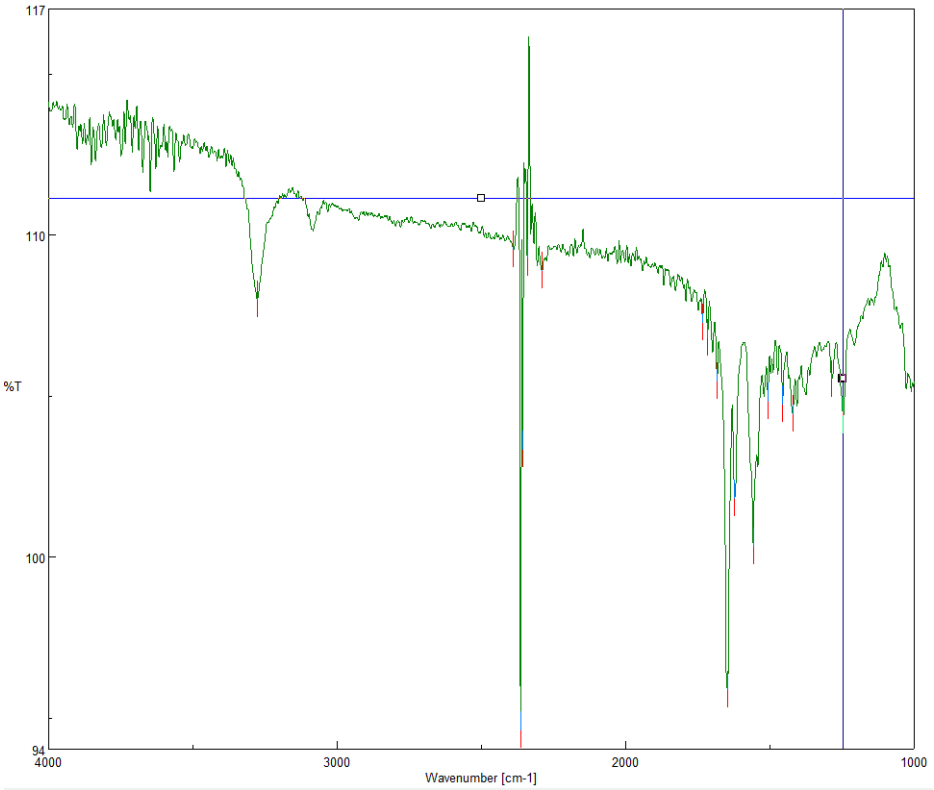

Figure S8c. IR spectrum (ATR) of the eliminated ligand (**12**).

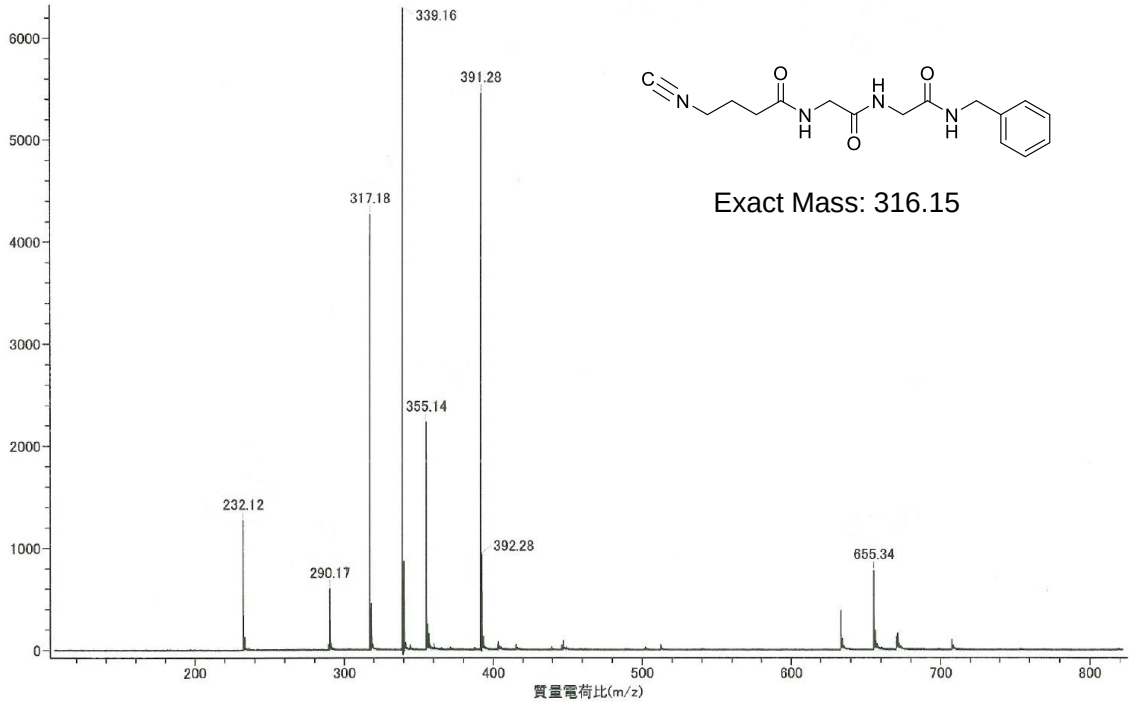

Figure S9a. ESI-MS spectrum of L_G' (**8b**).

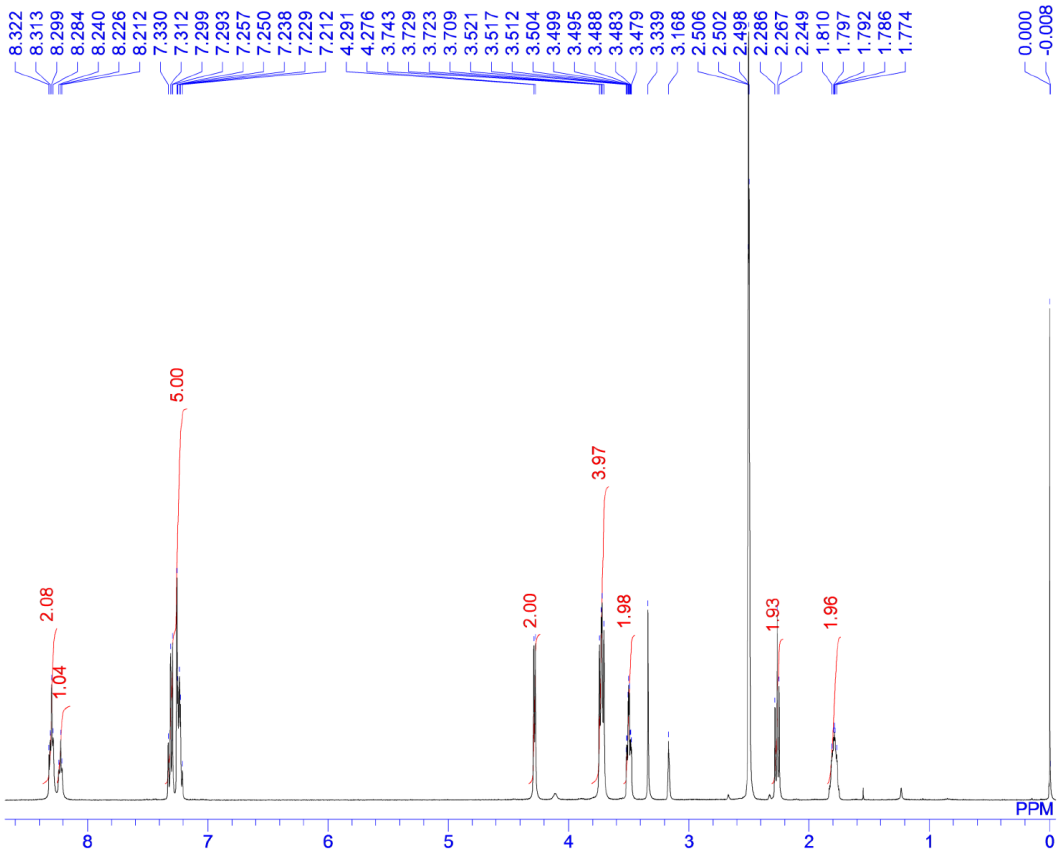

Figure S9b. ^{1}H NMR spectrum of L_G' (**8b**) in DMSO-d_6.

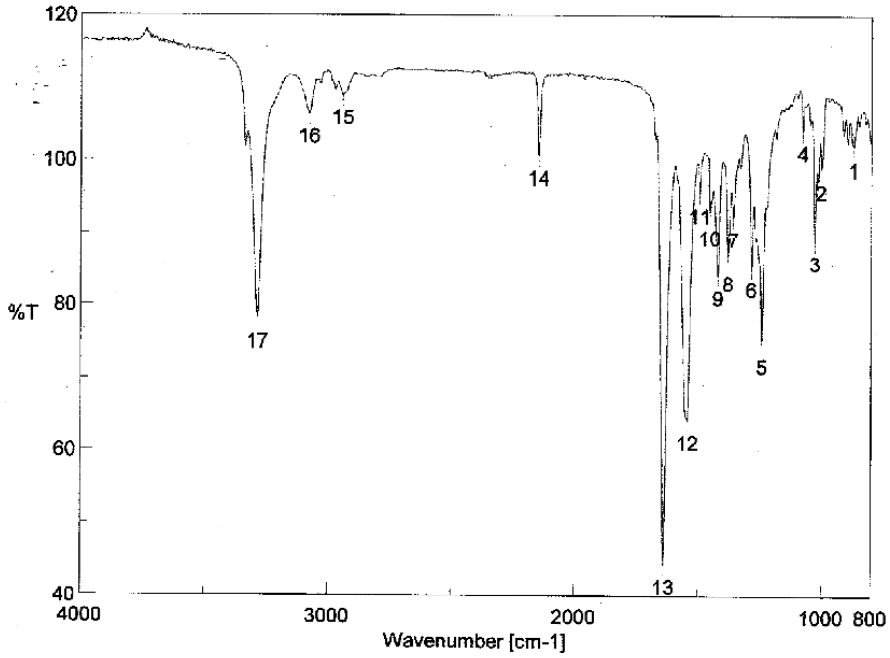

Figure S9c. IR spectrum (ATR) of L_G' (**8b**).

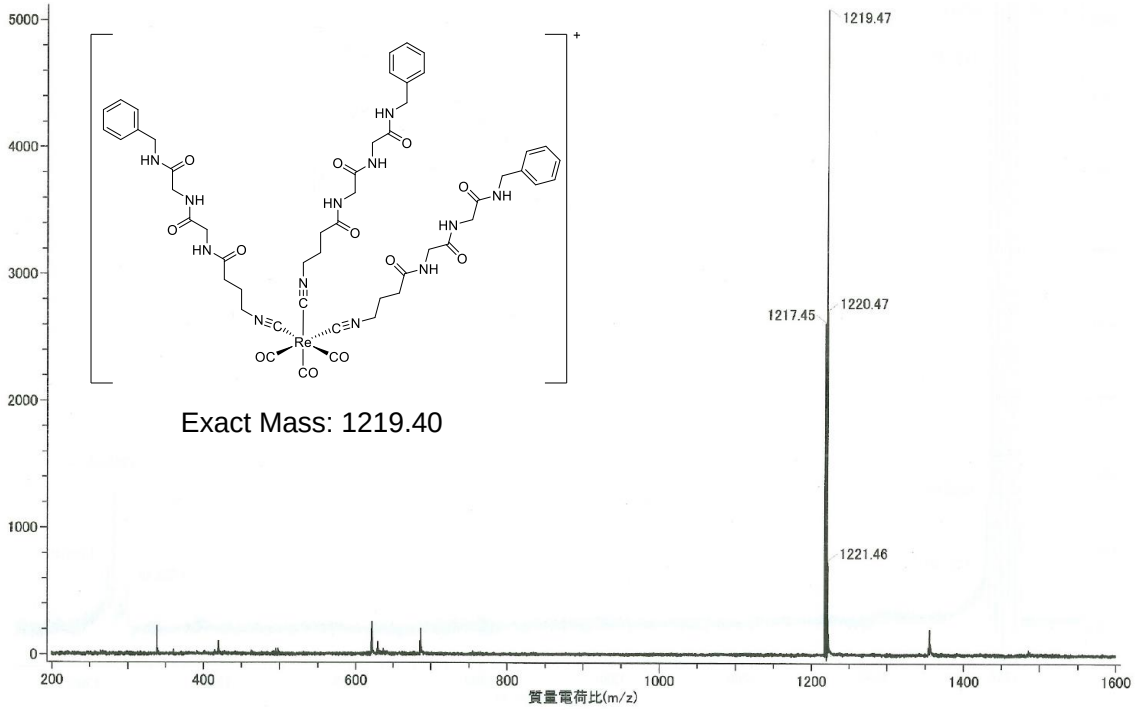

Figure S10a. ESI-MS spectrum of $[^{185/187}Re(CO)_3(L_G')_3]^+$ (**10**).

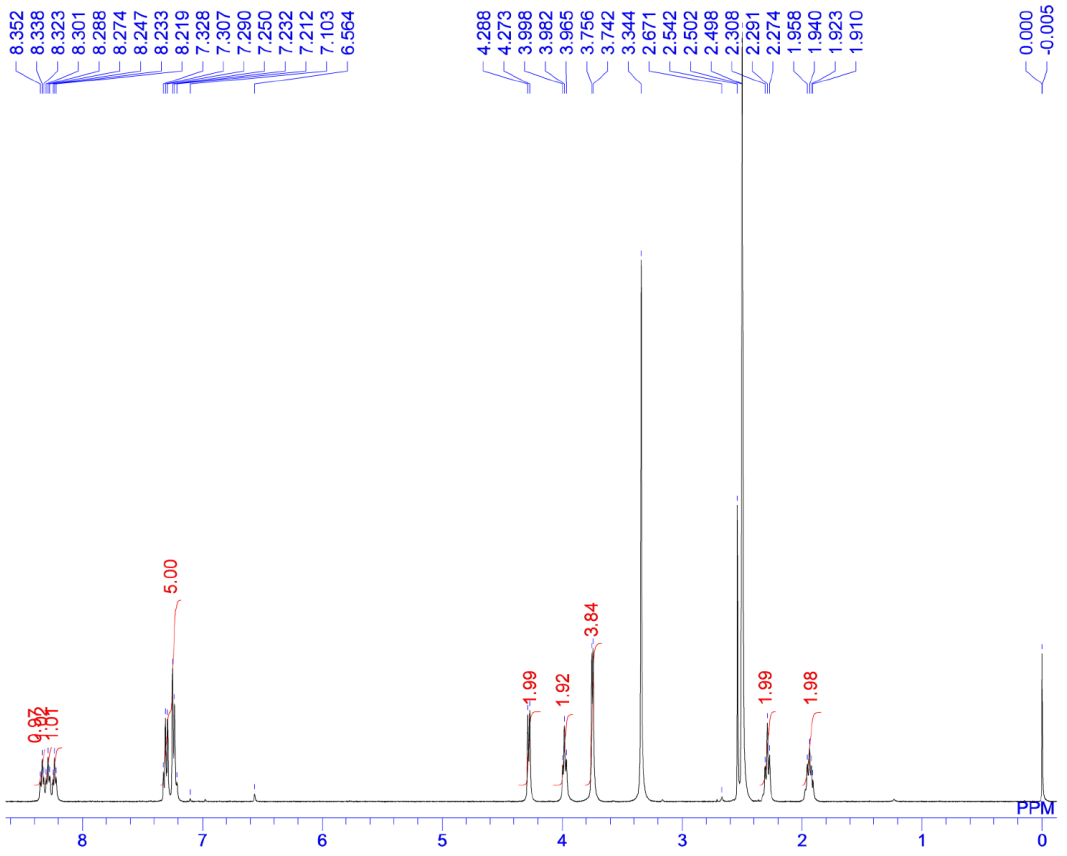

Figure S10b. ^{1}H NMR spectrum of $[^{185/187}Re(CO)_3(L_G')_3]^+$ (**10**) in DMSO-*d*$_6$.

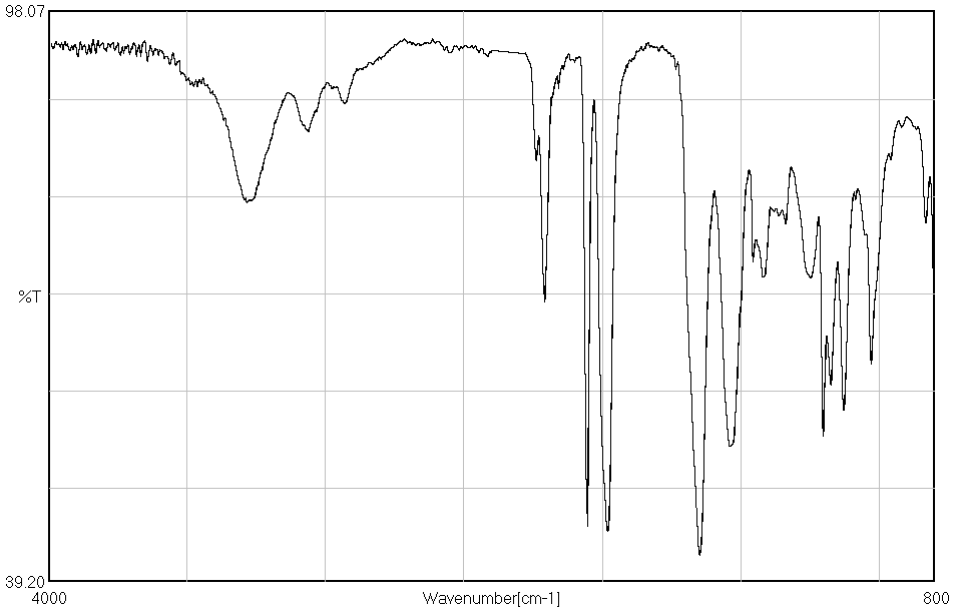

Figure S10c. IR spectrum (ATR) of $[^{185/187}Re(CO)_3(L_G')_3]^+$ (**10**).

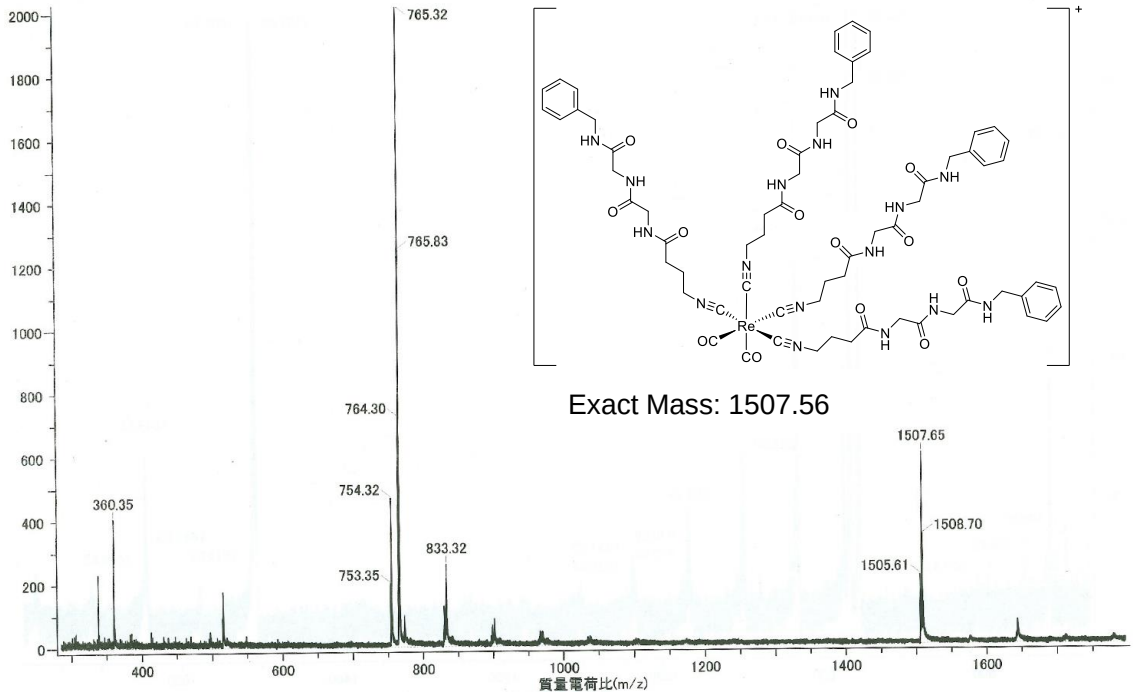

Figure S11a. ESI-MS spectrum of $[^{185/187}Re(CO)_2(L_G')_4]^+$ (**11**).

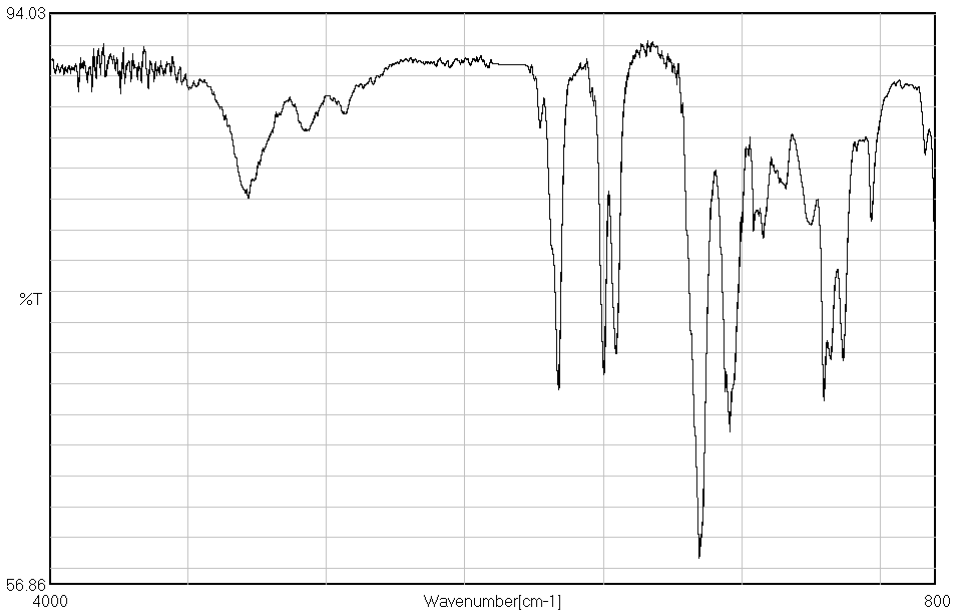

Figure S11b. IR spectrum (ATR) of $[^{185/187}Re(CO)_2(L_G')_4]^+$ (**11**).

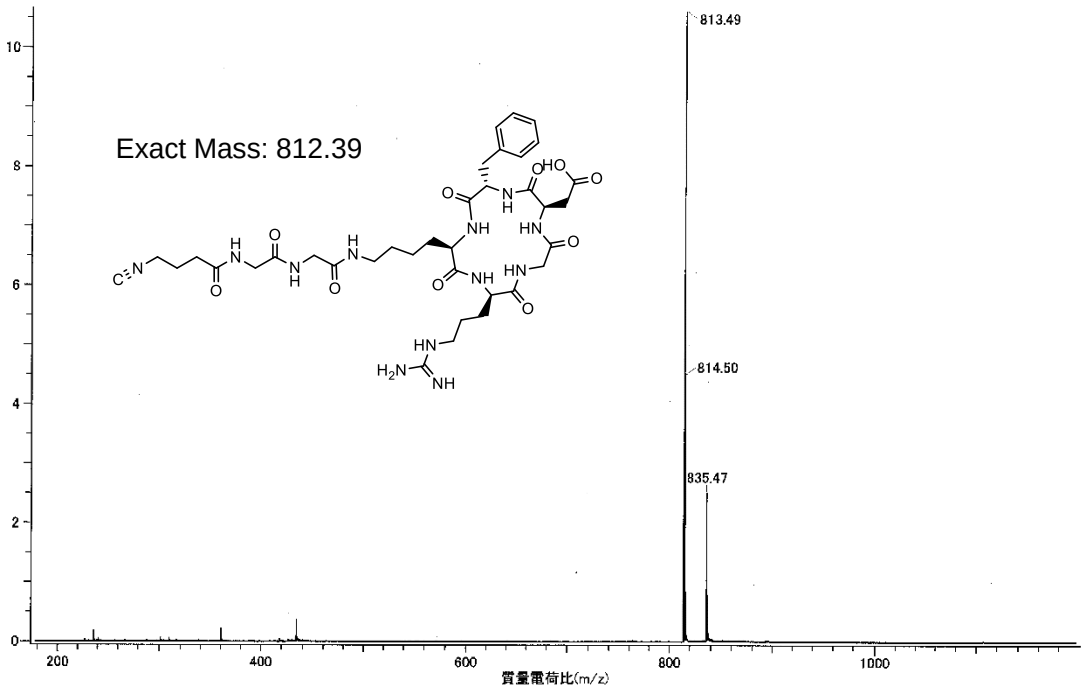

Figure S12a. ESI-MS spectrum of L_G (**16**).

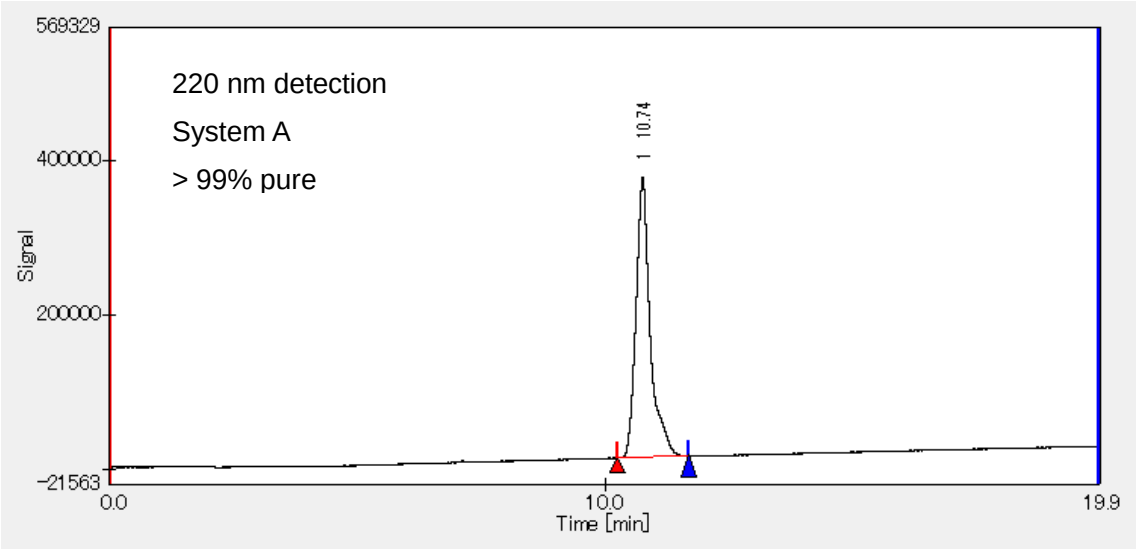

Figure S12b. HPLC chromatogram of L_G monitored at 220 nm using system 10, which showed >95% purity.

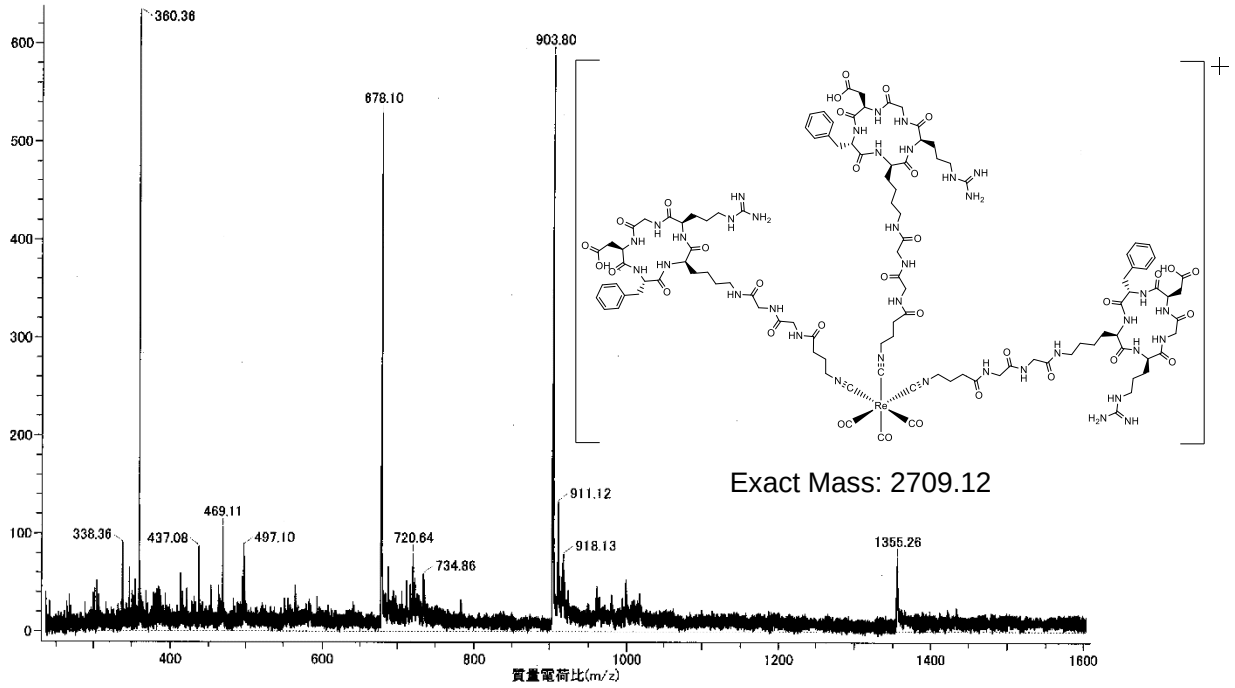

Figure S13a. ESI-MS spectrum of $[^{185/187}Re(CO)_3(L_G)_3]^+$ (**17**).

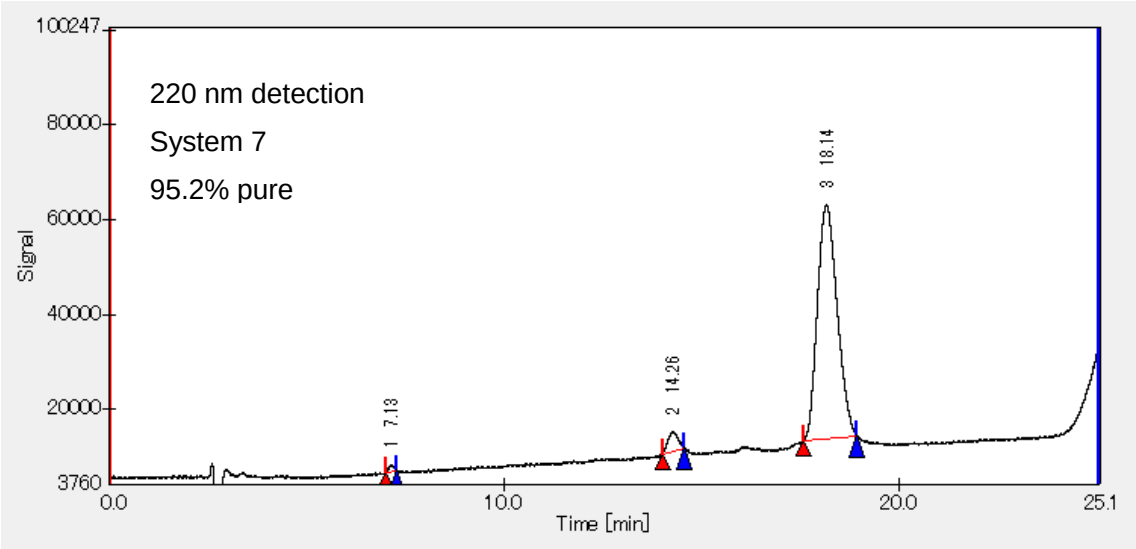

Figure S13b. HPLC chromatogram of $[^{185/187}Re(CO)_3(L_G)_3]^+$ monitored at 220 nm using system 7, which showed >95% purity.

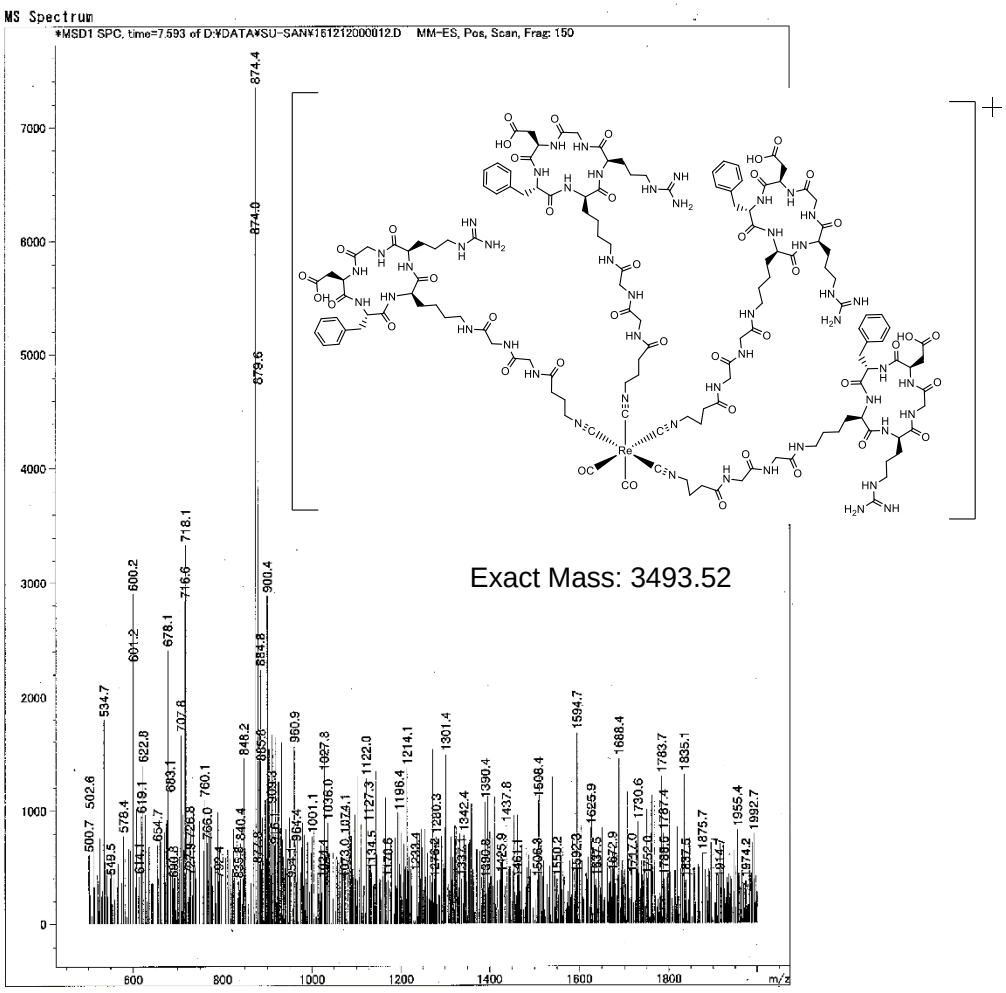

Figure S14a. ESI-MS spectrum of $[^{185/187}Re(CO)_2(L_G)_4]^+$ (**18**).

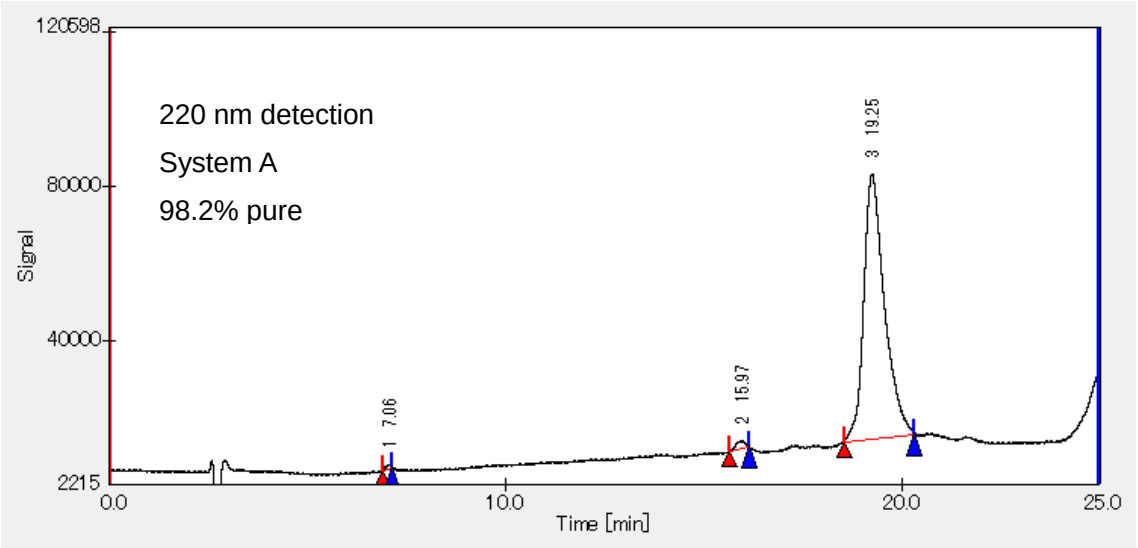

Figure S14b. HPLC chromatogram of $[^{185/187}Re(CO)_2(L_G)_4]^+$ monitored at 220 nm using system 7, which showed >95% purity.